DISCRETE AND CONTINUOUS
DYNAMICAL SYSTEMS
Volume **26**, Number **4**, April **2010**

doi:10.3934/dcds.2010.26.1419

pp. **1419–1440**

MODELING AND SIMULATION OF SWITCHINGS IN FERROELECTRIC LIQUID CRYSTALS

Jinhae Park, Feng Chen and Jie Shen

Department of Mathematics
Purdue University, 150 N. University Street
West Lafayette, IN 47907-2067, USA

Abstract. Mathematical modeling and numerical simulation of smectic C liquid crystals which possess the spontaneous polarization are considered in this paper. In particular, the model allows for a system with a zero net polarization which is one of the ubiquitous systems of the polarized liquid crystals. Theoretical and numerical investigations are conducted to study effects of the energy associated with the polarization, switching patterns between two uniform states by an externally applied field and random noise, as well as a relation between polarization and applied field near the phase transition from the smectic A and smectic C.

1. **Introduction.** We study in this paper the role of the energy associated with the polarization in smectic C liquid crystals. We mainly deal with the total energy of liquid crystals confined between two plates, and study properties of the energy in connection with physical phenomena.

Upon lowering temperature from the isotropic phase, we obtain the nematic phase in which the molecules tend to align along their long axes. In this case, the average long axis of the molecules defines the molecular director $\mathbf{n}$. With further cooling, there is locally a one-dimensional formation of layers with the director $\mathbf{n}$ being parallel to the layer normal, and the SmA phase emerges. The SmC phase can be obtained by lowering temperature from the SmA phase. In addition to the one-dimensional layer structure, in the SmC phase the molecules are tilted away from the layer normal, but free to rotate around it. We describe the SmC phase by the director $\mathbf{n}$ and the complex field $\psi = \rho e^{i\omega}$: level sets of the phase function ω correspond to the smectic layers and ρ to centers of mass of the molecules. If molecules are chiral in the SmC phase (labeled the SmC^*), the molecules rotate around the layer normal in a helical fashion. In SmC^* phase, there is also a spontaneous polarization field $\mathbf{P}$ in each layer due to the loss of mirror symmetry [8]. In this case, it is observed that the field $\mathbf{P}$ tends to perpendicular to both the director and layer normal, i.e. $\mathbf{P} = b_0\mathbf{n} \times \nabla\omega$ for constant b_0. The helical structure in the SmC^* phase can be suppressed by interactions with the surfaces of bounding plates in a thin cell (SSFLC) with $\mathbf{P}$ being perpendicular to the bounding plates. In the bent core molecules, a local uniform packing direction of the molecules within

2000 *Mathematics Subject Classification.* Primary: 76A15, 82D45; Secondary: 35Q35, 65M70, 65N35.

Key words and phrases. Antiferroelectric, Electrostatic, Equilibrium, Ferroelectric, Legendre collocation, Polarization, Smectic C, Switching.

This work is partially supported by NSF grants DMS-0456286, DMS-0610646 and AFOSR grant FA9550-08-1-0416.

layers determines the direction of the polarization field $\mathbf{P}$ (cf. Section 1 in [14]). Hereafter, we shall use ferroelectric liquid crystals to denote the SmC^* and bent core molecules.

In ferroelectric liquid crystals, two fundamental types are found: ferroelectric and antiferroelectric phases. In ferroelectric phases, all the polarization vectors point in the same direction, resulting in a nonzero net polarization. In antiferroelectric phases (SmC_A^*), the polarization vectors in subsequent layers point in the opposite directions by rotating 180° around the layer normal from one layer to the next, inducing a zero net polarization. It is also observed in the literature that mixed states of ferro-and antiferroelectric phases are possible in appropriate temperature ranges [21, 28]. This is responsible for the observations of multiple periodic phases with a stripe texture indicating that the layers are locally flat and parallel [15, 26]. Most of the known SmC_A^* phase appear at lower temperature than ferroelectric ones, which is opposite to the situation in solid state [19]. In a SSFLC, the SmC_A^* phase exhibits zero net polarization in the absence of applied fields. Upon application of an applied field (above a small threshold field), switching to a ferroelectric state takes place, reminiscent of SSFLC bistable switching in the SmC^*. With the removal of the applied field the molecules reorient to stabilize the system with a zero net polarization. This is the signature of existing small energy barriers between antiferroelectric and ferroelectric states resulting in a fast switching. In this case, switching between two ferroelectric states always undergoes antiferroelectric state. This induces a typical antiferroelectric hysteresis loop between polarization and applied field [3]. It is analogous to the situation in ferroelectric solids where a material in the cubic phase possesses zero polarization corresponding to antiferroelectric phase, particularly in the perovskite family. The cubic phase can be transformed into ferroelectric phases (tetragonal, orthorhombic and rhombohedral phases) by applied electric fields [4]. This leads us to include the following term in the Ginzburg-Landau energy associated with the polarization as considered in [28]:

$$a_1|\mathbf{P}|^2 + a_{11}|\mathbf{P}|^4 + a_{111}|\mathbf{P}|^6,$$

with a_1, a_{11}, and a_{111} being constants. From now on, we abuse notation to denote by antiferroelectric phase the system of a ferroelectric liquid crystal allowing for $\mathbf{P} = 0$ locally.

In this paper, we restrict ourselves to the system of a liquid crystal confined between two plates with uniform layer structures. We mainly focus on the antiferroelectric phases whose mathematical properties were not well studied in the literature, and investigate the minimizers of the governing energy functional in a thin domain. More specifically, we study how different energy terms affect on the structures of liquid crystal molecules in the system and establish numerical computations in order to understand the role of coefficients of the energy and random noise.

This paper is organized as follows. In Section 2, we introduce the total energy functional of ferroelectric liquid crystals accounting for mixture of ferroelectric and antiferroelectric phases. We then discuss the energy with the bookshelf geometry in Section 3. In Section 4, we study equilibrium solutions of the energy in the SmC^* phase. By the standard theories of bifurcations, we prove that surface energy interaction results in periodic equilibrium configurations nucleating from a ferroelectric state. These periodic solutions allow sharp interfaces at finite points when the thickness of the sample approaches zero. In other words, liquid crystal

molecules at these points rotate rapidly around the layer normal by π (see Figure 1). We then study minimizers of the energy functional focusing on the electrostatic energy in Section 5. Using the Young measure argument, we prove that the electrostatic energy favors fine structure of polarization in order to lower the total energy. These results are responsible for existence of mixture of two uniform states appearing in the physics literature [19, 22], resulting in a possibility of antiferroelectric state for an equilibrium state. In order to study the role of Ginzburg-Landau energy, we consider in Section 6 the system near the phase transition between the SmA and ferroelectric SmC phases. In the antiferroelectric phase, we note that the molecules exhibit a double hysteresis loop between polarization and applied fields, which agrees qualitatively with experimental data reported in [3]. We consider in Section 7 numerical simulations of the switching problem. In order to account for the presence of random noise due to impurities or thermal noise in the system, we add a stochastic term to the model, and use the Wentzell-Freidlin theory [11] to reformulate the problem as a minimization of the action functional. Then, we adapt the L-BFGS method (cf. [29]) coupled with a spectral discretization in space-time to simulate optimal switching patterns between two ferroelectric states. In Section 8, we present numerical approximations for local minimizers with an emphasis on the role of spontaneous twist and bend. We conclude with some remarks in the final section.

2. **Energy functional.** In this section, we discuss the energy functional for ferroelectric liquid crystals. The total energy functional of the continuum model for a system of a liquid crystal occupying a domain Ω is given by

$$\mathcal{E} = \int_\Omega \{F_N + F_{Sm} + F_P + F_E\}\, d\mathbf{x} + \int_{\partial\Omega} F_S\, dS - \frac{1}{2}\varepsilon_0 \int_{\mathbf{R}^3\setminus\Omega} |\mathbf{E}|^2\, d\mathbf{x} \tag{1}$$

subject to the Maxwell's equations

$$\begin{cases} -\nabla\cdot[(\varepsilon_\perp \chi_\Omega + \varepsilon_0 \chi_{\mathbf{R}^3\setminus\Omega})\mathbf{E})] = \nabla\cdot(\mathbf{p}\chi_\Omega) \text{ in } \mathbf{R}^3, \\ \nabla\times\mathbf{E} = 0 \text{ in } \mathbf{R}^3, \end{cases} \tag{2}$$

where $\varepsilon_\perp > 0, \varepsilon_0 > 0$, χ_Ω is the characteristic function in Ω, i.e. $\chi_\Omega(\mathbf{x}) = 1$ for $\mathbf{x}\in\Omega$ and 0 otherwise and

$$\begin{aligned}
F_N &= K_1(\nabla\cdot\mathbf{n})^2 + K_2(\mathbf{n}\cdot\nabla\times\mathbf{n} + \tau)^2 + K_3|\mathbf{n}\times(\nabla\times\mathbf{n}) - \gamma_0\mathbf{P}|^2 \\
&\quad + (K_2 + K_4)(tr(\nabla\mathbf{n})^2 - (\nabla\cdot\mathbf{n})^2), \\
F_{Sm} &= D(\mathbb{D}^2\Psi)(\mathbb{D}^2\Psi)^* + [C_{||}n_in_j + C_\perp(\delta_{ij} - n_in_j)](\mathbb{D}_i\Psi)(\mathbb{D}_j\Psi)^* \\
&\quad + r|\Psi|^2 + \frac{g}{2}|\Psi|^4, \\
F_P &= B|\nabla\mathbf{P}|^2 + K_c\Big[(\mathbf{n}\times\nabla\omega\cdot\mathbf{P})^2(\mathbf{n}\cdot\nabla\omega)^2 - \chi_0^2|\mathbf{P}|^2|\nabla\omega|^4\Big]^2 \\
&\quad + a_1|\mathbf{P}|^2 + a_{11}|\mathbf{P}|^4 + a_{111}|\mathbf{P}|^6, \\
F_S &= \Big(1 - \omega_n(\mathbf{n}\cdot\nu)^2\Big) + \Big(1 - \frac{\omega_p}{P_0}(\mathbf{P}\cdot\nu)\Big) + \Big(1 - \frac{\omega_r}{P_0^2}(\mathbf{P}\cdot\nu)^2\Big), \\
F_E &= -\frac{1}{2}\varepsilon_\perp|\mathbf{E}|^2 - \mathbf{P}\cdot\mathbf{E}.
\end{aligned}$$

The physical meanings of these energies are described below.

The energy F_N is the Oseen-Frank energy for the director field $\mathbf{n}$ [8], taking into account the flexoelectric effect. The classical Oseen-Frank energy for nematic

liquid crystals corresponds to the case that $\gamma_0 = 0$. The constant τ is the twist for cholesteric (chiral) liquid crystals depending on the material and the natural pitch is $\frac{2\pi}{\tau}$.

The smectic energy F_{Sm} [20] is obtained from the original Chen-Lubensky model in [7] by taking isotropic term $D(\mathbb{D}^2\Psi)(\mathbb{D}^2\Psi)^*$ instead of $D_\perp(\delta_{ij} - n_i n_j)(\delta_{kl} - n_k n_l)(\mathbb{D}_i\mathbb{D}_j\Psi)(\mathbb{D}_k\mathbb{D}_l\Psi)^*$, where $\mathbb{D} \equiv \nabla - iq\mathbf{n}$, q is the modulation wave number of the smectic layer, and $r = a(T - T^*), a > 0$; here T denotes the (constant) temperature of the material and T^* is the transition temperature from nematic to smectic. The smectic A phase corresponds to the case of $C_\perp > 0$. But in the smectic C phase, the constant $C_\perp$ could be negative so that $D(> 0)$-term is introduced to obtain coercivity of the energy. The de Gennes model for the chiral SmA corresponds to the case that $C_\parallel - C_\perp = 0$ and $D = 0$. In the case that $|\Psi|$ is constant (say $|\Psi| = 1$), we rewrite F_{Sm} as

$$F_{Sm} = D(\Delta\omega - q\nabla\cdot\mathbf{n})^2 + D\left(|\nabla\omega - q\mathbf{n}|^2 + \frac{C_\perp}{2D}\right)^2 \tag{3}$$
$$+C_a(\nabla\omega\cdot\mathbf{n} - q)^2 + \left(r + \frac{g}{2} - \frac{C_\perp^2}{2D}\right),$$

where $C_a = C_\parallel - C_\perp$. If C_a is large, then $\mathbf{n}$ tends to tilt at a definite angle to the layer normal.

The energy F_P is the energy associated with the polarization $\mathbf{P}$, where P_0 is the typical length of the polarization vector in the system. The K_c term is due to molecular packing between the smectic layers. A slightly different form of this term was considered in [2]. This can be formally justified by the interaction between polarization $\mathbf{P}$ and pseudo-vector $(\mathbf{n}\cdot\mathbf{k})(\mathbf{n}\times\mathbf{k})$ from the viewpoint of the Landau model [22, 23]. For this, the energy of polar and nonpolar effects is given by

$$-\alpha(\mathbf{n}\cdot\mathbf{k})(\mathbf{n}\times\mathbf{k}\cdot\mathbf{p}) + \beta(\mathbf{n}\cdot\mathbf{k})^2(\mathbf{n}\times\mathbf{k}\cdot\mathbf{p})^2, \tag{4}$$

where $\mathbf{k} = \frac{\nabla\omega}{|\nabla\omega|}, \mathbf{p} = \frac{\mathbf{P}}{|\mathbf{P}|}, \alpha > 0, \beta > 0$. After dividing (4) by β we express the energy as

$$[(\mathbf{n}\cdot\mathbf{k})(\mathbf{n}\times\mathbf{k}\cdot\mathbf{p}) - \chi_0]^2 - \frac{\alpha^2}{4\beta}, \tag{5}$$

where $\chi_0 = \frac{\alpha}{2\beta}$. From the first term in (5), we obtain the penalty term

$$\Big[(\mathbf{n}\cdot\nabla\omega)(\mathbf{n}\times\nabla\omega\cdot\mathbf{P}) - \chi_0|\nabla\omega|^2|\mathbf{P}|\Big]^2. \tag{6}$$

Since almost all systems of bent-core molecules allow for both handedness of three vectors, $\{\mathbf{n}, \nabla\omega, \mathbf{P}\}$, the K_c-term is introduced

$$K_c\Big[(\mathbf{n}\cdot\nabla\omega)^2(\mathbf{n}\times\nabla\omega\cdot\mathbf{P})^2 - \chi_0^2|\nabla\omega|^4|\mathbf{P}|^2\Big]^2. \tag{7}$$

We note that this term vanishes at $\mathbf{P} = 0$ and the constant K_c is generally large [2]. The last three terms in F_P is a typical Ginzburg-Landau energy. The first constant a_1 depends on the temperature. Suppose that $a_{11} > 0$ and $a_{111} = 0$. In this case, polar material(ferroelectric) corresponds to $a_1 < 0$; nonpolar material to $a_1 > 0$. If $a_1 < 0$, then we write

$$a_1|\mathbf{P}|^2 + a_{11}|\mathbf{P}|^4 = a_{11}\left(|\mathbf{P}|^2 + \frac{a_1}{2a_{11}}\right)^2 - \frac{a_1^2}{4a_{11}}.$$

In the case that a_{11} is negative, $a_{111}(>0)$-term should be included in order for the system to have a finite energy. Then we get

$$a_1|\mathbf{P}|^2 + a_{11}|\mathbf{P}|^4 + a_{111}|\mathbf{P}|^6 = a_{111}|\mathbf{P}|^2\left[\left(|\mathbf{P}|^2 + \frac{a_{11}}{2a_{111}}\right)^2 - \gamma\right],$$

where $\gamma = \frac{(a_{11}^2 - 4a_1 a_{111})}{4a_{111}^2}$.

This term allows for coexistence (mesophase) of polar and nonpolar states of the material. We note that nonpolar state corresponds to antiferroelectric state. We define g as

$$g(\mathbf{P}) = \begin{cases} \frac{1}{4\eta^2}(|\mathbf{P}|^2 - P_0^2)^2, & \text{ferroelectric phase,} \\ \frac{1}{6\eta^2}|\mathbf{P}|^2((|\mathbf{P}|^2 - P_0^2)^2 - \gamma), & \text{antiferroelectric phase,} \end{cases} \tag{8}$$

where $\eta \neq 0$, P_0 is the typical length of $\mathbf{P}$, and γ depends on the temperature.

The anchoring energy F_S is the typical Rapini-Papoular surface energy. The constants ω_n, ω_p, and ω_r are material constants [8, 19, 22]. The energy F_E is the electrostatic energy. We refer the reader to [25] for more details about this energy.

Throughout this paper, we assume that the constitutive parameters satisfy

$$\begin{cases} D > 0, C_\perp < 0, C_a > 0, r < 0, g > 0, \\ K_c > 0, \chi_0 \neq 0, \eta \neq 0, \tau \geq 0, B > 0, \\ c_1 \geq K_2 + K_4, \min\{K_1, K_2, K_3\} \geq K_2 + K_4, K_4 \leq 0. \end{cases} \tag{9}$$

The inequalities in the first row correspond to the SmC phase and the inequalities in the third row are necessary conditions for coercivity of the energy.

Remark 1. It follows from (3) [25] that the ground state of $F_N + F_{Sm}$ is given by

$$\begin{cases} \omega = \frac{qz}{c}, \quad \mathbf{n}^* = a\left(\cos\frac{\tau z}{a^2}\mathbf{e}_1 + \sin\frac{\tau z}{a^2}\mathbf{e}_2\right) + c\mathbf{e}_3, \\ \mathbf{P}^* = \frac{c\tau}{a\gamma_0}\left(\sin\frac{\tau z}{a^2}\mathbf{e}_1 - \cos\frac{\tau z}{a^2}\mathbf{e}_2\right), \\ a = \sin\theta_c, \quad c = \cos\theta_c, \quad \tan^2\theta_c = \frac{|C_\perp|}{2Dq^2}. \end{cases} \tag{10}$$

3. **Energy in the bookshelf geometry.** The total energy described in the last section is too complicated for detailed study so that we consider, for the rest of the paper, a bounded domain Ω confined between two plates, and restrict ourselves to the case that ρ is constant (say $\rho = 1$). Suppose that D, C_a, and $C_\perp$ satisfy $0 < \frac{|C_\perp|}{2Dq^2} \leq 1$. We further assume the following bookshelf geometry:

$$\omega = kz, \quad \tan^2\theta_c = \frac{|C_\perp|}{2Dq^2}, \quad \nabla\omega \cdot \mathbf{n} = |\nabla\omega|\cos\theta_c = q. \tag{11}$$

As seen in Remark 1, this geometry corresponds to the local smectic layer structure in the bulk. We then approximate $F_{Sm} + F_N$ by

$$\begin{aligned} F_n = {} & (K_1 + Dq^2)(\nabla\cdot\mathbf{n})^2 + K_2(\mathbf{n}\cdot\nabla\times\mathbf{n} + \tau)^2 + K_3|\mathbf{n}\times(\nabla\times\mathbf{n}) - \gamma_0\mathbf{P}|^2 \\ & + (K_2 + K_4)(tr(\nabla\mathbf{n})^2 - (\nabla\cdot\mathbf{n})^2) + \frac{1}{\epsilon^2}\left[(n_3 - c)^2 + \left(n_1^2 + n_2^2 - a^2\right)^2\right], \end{aligned}$$

where $\epsilon > 0$, $a = \sin\theta_c, c = \cos\theta_c$, and $\mathbf{n} = (n_1, n_2, n_3)$. It is easy to see that $\int_\Omega (F_N + F_{Sm})\,d\mathbf{x}$ and $\int_\Omega F_n\,d\mathbf{x}$ have the same ground states.

In the following, we consider the total energy functional

$$\mathcal{E}(\mathbf{n}, \mathbf{P}) = \int_\Omega \{F_n + F_P + F_\varphi\} - \frac{1}{2}\int_{\mathbf{R}^3\setminus\Omega} \varepsilon_0|\nabla\varphi|^2\,d\mathbf{x} + \int_{\partial\Omega} F_{surf}(\mathbf{n}, \mathbf{P}, \nu)\,ds,$$

where

$$F_p = B|\nabla \mathbf{P}|^2 + K_c k^8 \left[(\mathbf{n}\times\mathbf{e}_3\cdot\mathbf{P})^2(\mathbf{n}\cdot\mathbf{e}_3)^2 - \chi_0^2|\mathbf{P}|^2\right]^2 + g(\mathbf{P}),$$
$$F_\varphi = -\frac{1}{2}\varepsilon_\perp|\nabla\varphi|^2 - \mathbf{P}\cdot\nabla\varphi,$$

and $\mathbf{E} = \nabla\varphi$ satisfies (2). We then define an admissible set

$$\mathcal{A} = \Big\{(\mathbf{n},\mathbf{P},\varphi)|\mathbf{n}\in W^{1,2}(\Omega,\mathbb{S}^2), \mathbf{P}\in W^{1,2}(\Omega,\mathbf{R}^3), \varphi\in W^{1,2}(\mathbf{R}^3), \\ ||\mathbf{P}||_\infty \le P_0, \text{ and } (\mathbf{n},\mathbf{P},\varphi) \text{ satisfy (2)}\Big\}.$$

Theorem 3.1. *There exists a minimizing triple* $(\bar{\mathbf{n}},\bar{\mathbf{P}},\bar{\varphi})\in\mathcal{A}$ *of* $\mathcal{E}$ *so that*

$$\mathcal{E}(\bar{\mathbf{n}},\bar{\mathbf{P}},\bar{\varphi}) = \inf_{(\mathbf{n},\mathbf{P},\varphi)\in\mathcal{A}} \mathcal{E}(\mathbf{n},\mathbf{P},\varphi) < M$$

for some $M > 0$.

The proof of the theorem follows from [25] with some minor changes. Moreover, $\bar{\mathbf{n}},\bar{\mathbf{P}}$ and $\bar{\varphi}$ are locally Hölder continuous on $\Omega\setminus Z$ for a subset Z of Ω with one dimensional Hausdorff measure zero [17].

For the rest of this paper, for simplicity we assume that

$$\Omega = \{(x,y,z)\in\mathbf{R}^3 : 0<x<d_1, 0<y<d_2, 0<z<d_3\},$$
$$K_1 + q^2 D = K_2 = K_3 = K > 0,\ K_4 = 0,\ B > 0.$$

Then F_n is given by

$$F_n = K|\nabla\mathbf{n}|^2 + 2K\tau(\mathbf{n}\cdot\nabla\times\mathbf{n}) - 2K\gamma_0(\mathbf{n}\times\nabla\times\mathbf{n}\cdot\mathbf{P}) \\ + \frac{1}{\epsilon^2}\left[(n_3-c)^2 + \left(n_1^2+n_2^2-a^2\right)^2\right] + K\gamma_0^2|\mathbf{P}|^2.$$

4. **Periodic configurations due to surface energy.** In this section, we discuss the effect of the surface energy in connection with a surface stabilized ferroelectric liquid crystal (SSFLC). In a very thin domain, we show that due to surface energy there exist finitely many periodic configurations which have sharp interfaces at finite points as the thickness approaches zero.

Let us assume that $d_2 = d_3 = l > 0$, $\omega_n < 0$, and $\omega_r > 0$. Choose admissible fields $\mathbf{n}$, $\mathbf{P}$ such that

$$\mathbf{n} = (a\cos\phi, a\sin\phi, c),\quad \mathbf{P} = P_0(\sin\phi, -\cos\phi, 0) = P_0\frac{\mathbf{n}\times\mathbf{e}_3}{|\mathbf{n}\times\mathbf{e}_3|},$$

where ϕ depends on y and z. Let

$$D_l = \{(y,z) : 0<y<l, 0<z<l\},$$

and we impose the Dirichlet boundary condition, $\phi = 0$ on ∂D_l, and ignore the electrostatic energy. After dividing $\mathcal{E}$ by d_1 we express the energy functional in term of ϕ (still labeled $\mathcal{E}$)

$$\mathcal{E}(\phi) = \int_{D_l}\left\{F_n + F_P - \frac{\omega_n a^2}{d_1}\cos^2\phi - \frac{\omega_r P_0^2}{d_1}\sin^2\phi\right\}d\mathbf{x}, \\ = \int_{D_l}\left\{(Ka^2 + BP_0^2)|\nabla\phi|^2 - \frac{1}{d_1}(\omega_r P_0^2 - \omega_n a^2)\sin^2\phi\right\}d\mathbf{x} + M,$$

for some M and $d\mathbf{x}$ denotes $dydz$.

Let

$$\bar{y} = \frac{y}{l}, \quad \bar{z} = \frac{z}{l}, \quad \bar{\mathcal{E}}(\phi) = \frac{1}{(a^2K + BP_0^2)} \left[\mathcal{E}(\phi) - M\right].$$

Write $\bar{\mathcal{E}}(\phi)$ in terms of $\bar{y}$ and $\bar{z}$, and drop the bars in order to obtain

$$\begin{cases} \mathcal{E}(\phi) = \int_{D_1} \left\{|\nabla\phi|^2 - \lambda \sin^2\phi\right\} d\mathbf{x}, \\ \phi = 0 \text{ on } \partial D_1, \end{cases}$$

where $\lambda = \frac{L^2(\omega_r P_0^2 - \omega_n a^2)}{d_1(a^2K + BP_0^2)}$. The corresponding Euler-Lagrange equation is

$$\begin{cases} -\Delta\phi - \lambda \sin 2\phi = 0 \text{ in } D_1, \\ \phi = 0 \text{ on } \partial D_1. \end{cases} \tag{12}$$

Let $\{\mu_k : 0 < \mu_1 < \mu_2 < \cdots < \mu_k < \cdots, k = 1, 2, ...\}$ be the set of eigenvalues of

$$\begin{cases} -\Delta\phi_k = \mu_k \phi_k \text{ in } D_1, \\ \phi_k = 0 \text{ on } \partial D_1, \end{cases}$$

where $||\phi_k||_{L^2} = 1$ for $k \in \mathbb{N}$.

Thanks to the results in [6, 9] we have the following theorem.

Theorem 4.1. *If $\lambda > \mu_1$ and ϕ_0 is a global minimizer, then $-\phi_0$ is also a global minimizer and $-\frac{\pi}{2} \le \phi_0 \le \frac{\pi}{2}$ in D_1. Furthermore, the Euler-Lagrange equation (12) admits a unique positive solution $\psi \in H^1(D_1) \cap C^{2,\delta}(D_1)$ satisfying $0 < \psi < \frac{\pi}{2}$ in D_1 where $0 < \delta \le 1$. If $\lambda > \mu_2$, then there are at least four nontrivial solutions. If $\lambda > \mu_k$, then there are at least k different nontrivial solutions. Furthermore, the unique positive solution ψ is a global minimizer for $\lambda > \mu_1$.*

Remark 2. The uniqueness of the positive solution in theorem 4.1 is true for all convex domain D_1 [9]. But it is still an open problem whether it is true for a general domain although there is a positive numerical evidence for a dumbbell-like domain. For more detail, we refer the reader to [9].

The results in Theorem 4.1 are consistent with a surface stabilized ferroelectric liquid crystal (SSFLC) [19]. In a SSFLC, the direction field prefers to tilt right ($\phi = \frac{\pi}{2}$) or left ($\phi = -\frac{\pi}{2}$) because of the surface energy. The two solutions $\pm\psi$ correspond to two ferroelectric states. If the thickness d_1 is small, the sample may exhibit non uniform structures other than $\pm\psi$ as proved in the previous theorem. In this case, application of an applied field parallel to $x-$axis causes a reorientation of the polarization, which leads to one of ferroelectric states (say ψ). This ferroelectric state remains unchanged upon the removal of the applied field because $\pm\psi$ are global minimizers. The other ferroelectric state is obtained by application of the field of opposite sign. This mechanism is known as *bistable switching*.

In the absence of applied fields, it is observed in the literature that the molecules in a SSFLC exhibit periodic structures by precession of the director 180° rotating around the layer normal [13]. In the following, we study these periodic solutions which depend on z. This leads to the problem

$$\begin{cases} \mathcal{E}(\phi) = \int_0^1 \left\{(\phi')^2 - \lambda \sin^2\phi\right\} dz, \\ \phi(0) = -\phi(1), \phi'(0) = \phi'(1) = 0. \end{cases} \tag{13}$$

Setting $u = 2\phi$, we find that u satisfies the Euler-Lagrange equation

$$\begin{cases} u'' + \lambda \sin u = 0 \text{ in } (0,1), \\ u(0) = -u(1), u'(0) = u'(1) = 0. \end{cases} \tag{14}$$

Define

$$X = \{u \in C^2[0,1] : u(0) = -u(1), u'(0) = u'(1) = 0\}, \quad Z = C[0,1].$$

Let $F : X \times \mathbf{R} \to Z$ be defined by $F(u,\lambda) = u'' + \lambda \sin u$. It is clear that $(0,\lambda)$ is a solution pair of $F(u,\lambda) = 0$. First we note that $D_u F(0,\lambda)\psi = 0, \psi \in X$ if and only if $\psi'' + \lambda\psi = 0 \in Z,\ \psi(0) = -\psi(1),\ \psi'(0) = \psi'(1) = 0$. It is easy to show that the boundary value problem has a solution $(\psi,\lambda), \lambda > 0, \psi \neq 0$ if and only if $\lambda = \lambda_k = (2k-1)^2\pi^2, k \in \mathbb{N}$ and ψ is a multiple of $\psi_k(s) = \cos[(2k-1)\pi s]$. So, $\dim\ker D_u F(0,\lambda_k) = 1$ for each $k \in \mathbb{N}$. Set $L_k = D_u F(0,\lambda_k)$.

Then $R(L_k) = \{v \in Z : \int_0^1 v(s)\psi_k(s)\,ds = 0\}$, and $Z_0 = span\{\psi_k\} = R(L_k)^\perp = \ker L_k^*$, because L_k is a self adjoint operator.

By the standard local and global bifurcation theorems [1, 12], it is easy to check that each point $(0,\lambda_k)$ is a pitchfork bifurcation point and there exists a global nontrivial solution branch of solutions emanating from $(0,\lambda_k)$. Let $\mathcal{S}_k$ be the set of all nontrivial solutions bifurcating from $(0,\lambda_k)$. Then for each $\lambda > \lambda_k$, there exists $u_\lambda^k \in \mathcal{S}_k$ satisfying (14). Moreover, u_λ^k has exactly $2k-1$ roots. Letting $\lambda \to \infty$ it is seen that $|u_\lambda^k(x)| \to \pi$ modulo 2π, *a.e.* $x \in [0,1]$. Hence, if $d_1 << l^2$, there exist at least M such solutions where M is the largest integer such that $(2M-1)^2\pi^2 \le M_0 \frac{l^2}{d_1}$, $M_0 = \frac{\omega_r P_0^2 - \omega_n a^2}{a^2 K + B P_0^2}$. This proves the existence of mixture of two ferroelectric states in a thin SSFLC due to surface interactions. This is responsible for the existence of multiple periodic solutions in switching between two ferroelectric states $\phi = \pm\frac{\pi}{2}$. It should be mentioned that these nontrivial solutions bifurcate from a ferroelectric phase $\phi = 0$ different from $\pm\frac{\pi}{2}$. We summarize as a lemma.

Lemma 4.2. *Let* $\lambda = \frac{l^2(\omega_r P_0^2 - \omega_n a^2)}{d_1(a^2 K + B P_0^2)}$. *Let* M *be the largest integer such that*

$$(2M-1)^2\pi^2 \le \lambda.$$

Then for each $1 \le k \le M$, *there exists at least one nontrivial solution* u_λ^k *of (14) such that* u_λ^k *has exactly* $(2k-1)$ *roots and* $|u_\lambda^k(x)| \to \pi$ *modulo* 2π *as* $\lambda \to \infty$ *for almost all* $x \in [0,1]$.

In Figure 1, we plot $u_\lambda^k (k = 1,2,3)$ for several values of λ. We see that $u_\lambda^k(x)$ approaches to $\pm\pi$ as we increase the values of λ except finite points.

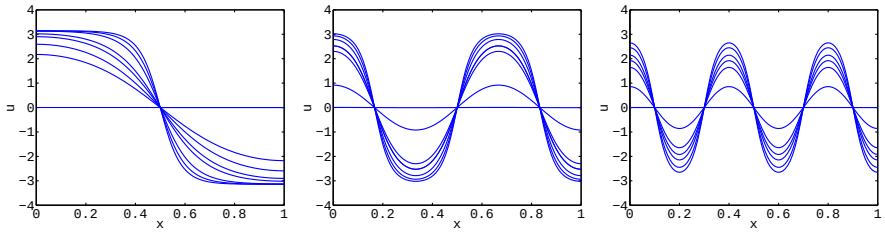

FIGURE 1. $\lambda = l\pi^2$, left: $l = 0.5, 2, 3, 5, 7, 16, 25, 36$; center: $l = 6, 10, 16, 25, 36, 49, 64$; right: $l = 10, 27, 36, 42, 49, 64, 81$.

5. **Electrostatic energy and fine structure.** In the present section, we study the effect of the electrostatic energy when the ratio of the elastic constants to the size of domain goes to zero. We assume that $\mathbf{n}$ depends on x and z, and that

$$\begin{cases} Ka^2 = BP_0^2 = K_0, \;\; d_1 = d_3 = L, \;\; d_2 = 1, \;\; \omega_n < 0, \;\; \omega_p = 0, \\ \omega_r > 0, \;\; \tau = 0, \;\; \gamma_0 = 0, \;\; \mathbf{n} = (au_1, au_2, c), \;\; \mathbf{P} = P_0(p_1, p_2, p_3). \end{cases} \tag{15}$$

It follows from the assumption (15) that the angle between $\mathbf{n}$ and the layer normal is fixed. Since $\tau = 0$ and $\gamma_0 = 0$, the molecules we consider here are not chiral and there is no flexoelectric effect.

Since

$$(\nabla \cdot \mathbf{n})^2 + |\nabla \times \mathbf{n}|^2 = a^2 |\nabla \mathbf{u}|^2,$$

the total energy functional reads

$$\begin{aligned} \mathcal{E}(\mathbf{u}, \mathbf{p}, \varphi) = \int_{[0,L]\times[0,L]} \left\{ F_n + F_P - \frac{\omega_n a^2}{2} n_1^2 - \frac{\omega_r}{2} P_0^2 p_1^2 \right\} dxdz \\ -\frac{1}{2} P_0 \int_{\mathbf{R}^2} \{\mathbf{p}\chi_{[0,L]\times[0,L]} \cdot \mathbf{E}\} \, dxdz, \end{aligned}$$

where $\mathbf{u} = (u_1, u_2)^t$, $\mathbf{p} = (p_1, p_2, p_3)^t$, and

$$\begin{aligned} F_n + F_P = K_0 |\nabla \mathbf{u}|^2 + K_0 |\nabla \mathbf{p}|^2 + \frac{1}{4\xi^2} P_0^4 (|\mathbf{p}|^2 - 1)^2 \\ + K_c k^8 P_0^4 \left[a^2 c^2 (u_2 p_1 - u_1 p_2)^2 - \chi_0^2 |\mathbf{p}|^2 \right]^2. \end{aligned}$$

Choose ξ, χ_0 such that $\frac{\chi_0}{ac} = 1, P_0^4 = \xi^2$ and set

$$\mathbf{u} = (\cos\phi, \sin\phi), \quad \beta = K_c k^8 P_0^4.$$

We scale y, z by $\frac{y}{L}, \frac{z}{L}$, and denote $\frac{K_0}{L^2}$ by ε^2. Replace F by $\frac{1}{L^2}(F + \frac{\omega_r}{2} P_0^2)$ to obtain

$$\begin{aligned} \mathcal{E}(\mathbf{u}, \mathbf{p}) = \int_\Omega \Big\{ \varepsilon^2 |\nabla \phi|^2 + \varepsilon^2 |\nabla \mathbf{p}|^2 + \beta \chi_0^4 \left[(p_1 \sin\phi - p_2 \cos\phi)^2 - |\mathbf{p}|^2 \right]^2 \\ + \frac{1}{4}(|\mathbf{p}|^2 - 1)^2 - \frac{\omega_n a^2}{2} \cos^2\phi + \frac{P_0^2 \omega_r}{2}(1 - p_1^2) \Big\} \, d\mathbf{x} - \frac{1}{2} P_0 \int_{\mathbf{R}^2} \mathbf{p}\chi_\Omega \cdot \mathbf{E} \, d\mathbf{x} \end{aligned}$$

subject to

$$-\nabla \cdot [(\varepsilon_\perp \chi_\Omega + \varepsilon_0 \chi_{\mathbf{R}^2 \setminus \Omega}) \nabla \varphi)] = \nabla \cdot (\mathbf{p}\chi_\Omega) \text{ in } \mathbf{R}^2, \tag{16}$$

where $\mathbf{E} = \nabla\varphi$, $d\mathbf{x} = dxdz$, and $\Omega = [0,1] \times [0,1]$.

Let $\mathcal{B}$ be a ball containing Ω and define

$$\begin{aligned} \tilde{\mathcal{A}} = \Big\{ (\phi, \mathbf{p}, \varphi) \;:\; (\phi, \mathbf{p}) \in W^{1,2}(\Omega, [-\pi/2, \pi/2]) \times W^{1,2}(\Omega, \mathbf{R}^3), \\ ||\mathbf{p}||_\infty \le 1, \varphi \in \mathcal{V} \text{ and } (\phi, \mathbf{p}, \varphi) \text{ satisfies (16)} \Big\}, \\ \mathcal{V} = \left\{ \varphi \;:\; \varphi\big|_{\mathcal{B}} \in W^{1,2}(\mathcal{B}, \mathbf{R}), \quad \nabla\varphi \in L^2(\mathbf{R}^2), \quad \int_{\mathcal{B}} \varphi \, d\mathbf{x} = 0 \right\}. \end{aligned}$$

We define inner product $< , >$ by

$$< u, v >= \int_{\mathcal{B}} uv \, d\mathbf{x} + \varepsilon_\perp \int_{\mathbf{R}^3} \nabla u \cdot \nabla v \, d\mathbf{x}.$$

By the direct method of calculus of variations, for each $\varepsilon > 0$ there exists a minimizer of $\mathcal{E}_\varepsilon$ on $\tilde{\mathcal{A}}$. From (16), we notice that φ is not a constant function so that

$$\min_{(\mathbf{u},\mathbf{p},\varphi)\in\tilde{\mathcal{A}}} \mathcal{E}_\varepsilon(\mathbf{u},\mathbf{p},\varphi) > 0 \text{ for } \varepsilon > 0.$$

In order to see the effect of electrostatic energy for a small ε, let us denote by ζ a smooth function in $C^\infty(\mathbf{R},[-1,1])$ satisfying

$$\zeta(t) = \begin{cases} -1 & \text{if } t \le 0, \\ 1 & \text{if } t \ge 1. \end{cases}$$

For fixed $0 \le \theta \le 1$ and $s \ge 3$, let

$$a_k = \frac{1}{2k} - \theta\left(\frac{1}{2k} - \frac{1}{k^s}\right) - \frac{1}{k^s}, \quad b_k = \frac{1}{2k} - \theta\left(\frac{1}{2k} - \frac{1}{k^s}\right),$$
$$c_k = \frac{1}{2k} + \theta\left(\frac{1}{2k} - \frac{1}{k^s}\right), \qquad d_k = \frac{1}{2k} + \theta\left(\frac{1}{2k} - \frac{1}{k^s}\right) + \frac{1}{k^s}.$$

For each k, let $h_k : \Omega \to [-1,1]$ be a periodic function in z with the period $\frac{1}{k}$ satisfying

$$h_k(x,z) = \begin{cases} -1 & \text{if } 0 \le z \le a_k, \\ \zeta\left(k^s(z-a_k)\right) & \text{if } a_k \le z \le b_k, \\ 1 & \text{if } b_k \le z \le c_k, \\ \zeta\left(k^s(d_k-z)\right) & \text{if } c_k \le z \le d_k, \\ -1 & \text{if } d_k \le z \le \frac{1}{k}. \end{cases}$$

Let

$$\phi_k(x,z) = \frac{\pi}{2}h_k(z), \quad \mathbf{p}_k(x,z) = \left(\sin\left(\frac{\pi}{2}h_k(z)\right), -\cos\left(\frac{\pi}{2}h_k(z)\right), 0\right).$$

It is not hard to see that

$$\int_\Omega \left\{|\nabla\phi_k|^2 + |\nabla\mathbf{p}_k|^2\right\} d\mathbf{x} \le Ck^{2s+1}\int_{-\infty}^{\infty} \zeta'(t)^2\, dt,$$
$$(\phi_k, \mathbf{p}_k) \rightharpoonup \left((2\theta-1)\frac{\pi}{2}, (2\theta-1)\mathbf{e}_1\right) \text{ in } L^2(\Omega),$$
$$f(\phi_k,\mathbf{p}_k) \to 0 \text{ in } L^1(\Omega),$$

where

$$f(\phi,\mathbf{p}) = \beta\chi_0^4\left[(p_1\sin\phi - p_2\sin\phi)^2 - |\mathbf{p}|^2\right]^2 + \frac{1}{4}(|\mathbf{p}|^2-1)^2 - \frac{\omega_n a^2}{2}\cos^2\phi + \frac{P_0^2\omega_r}{2}(1-p_1^2).$$

Let φ_k be the solution of (16) corresponding to $\mathbf{p}_k\chi_\Omega$. It is standard to show that $\varphi_k \rightharpoonup 0$ in $\mathcal{V}$ so that $\varphi_k \to 0$ in $L^2(\Omega)$ and $\varphi_k|_{\partial\Omega} \to 0$ in $L^2(\partial\Omega)$. This implies that

$$\frac{1}{2}\int_\Omega \mathbf{p}_k\cdot\nabla\varphi_k\, d\mathbf{x}$$
$$= -\frac{1}{2}\int_\Omega \nabla\cdot\mathbf{p}_k\varphi_k\, d\mathbf{x} + \frac{1}{2}\int_{\partial\Omega}\varphi_k\mathbf{p}_k\cdot\nu\, dS \to 0 \quad \text{as } j \to 0.$$

Furthermore, by the choice of $\varepsilon_k = \frac{1}{k^{s+1}}$ we have

$$\varepsilon_k^2\int_\Omega \left\{|\nabla\mathbf{u}_k|^2 + |\nabla\mathbf{p}_k|^2\right\} d\mathbf{x} \to 0 \text{ as } k \to \infty.$$

Since $\mathcal{E}_{\varepsilon_k}(\mathbf{u},\mathbf{p},\varphi) > 0$ from (16), we get

$$0 = \lim_{k\to\infty} \mathcal{E}_{\varepsilon_k}(\mathbf{u}_k,\mathbf{p}_k,\varphi_k) \geq \lim_{k\to\infty} \min_{(\mathbf{u},\mathbf{p},\varphi)\in\tilde{\mathcal{A}}} \mathcal{E}_{\varepsilon_k}(\mathbf{u},\mathbf{p},\varphi) \geq 0.$$

Hence, we conclude the following lemma:

Lemma 5.1. *If $(\mathbf{u}_\varepsilon,\mathbf{p}_\varepsilon,\varphi_\varepsilon) \in \tilde{\mathcal{A}}$ is a minimizer of $\mathcal{E}_\varepsilon$, then*

$$\lim_{\varepsilon\to 0} \mathcal{E}_\varepsilon(\mathbf{u}_\varepsilon,\mathbf{p}_\varepsilon,\varphi_\varepsilon) = 0.$$

Furthermore, we have the following:

Theorem 5.2. *Let $\{(\phi^\varepsilon,\mathbf{p}^\varepsilon,\varphi^\varepsilon)\}$ be a minimizing sequence. Then there exists a subsequence, still denoted by the same notation, such that $\{(\phi^\varepsilon,\mathbf{p}^\varepsilon)\}$ converges weakly star to $(\bar\phi,\bar{\mathbf{p}})$ in $L^\infty(\Omega)$ where $(\bar\phi(\mathbf{x}),\bar{\mathbf{p}}(\mathbf{x})) = \frac{1}{2}\delta_{(-\pi/2,\mathbf{e}_1)}(\mathbf{x}) + \frac{1}{2}\delta_{(\pi/2,-\mathbf{e}_1)}(\mathbf{x})$.*

Proof. The proof of this theorem is almost the same as in [16] for ferromagnetic materials. For the completeness, we sketch the proof in the following. Let $(\phi^\varepsilon,\mathbf{p}^\varepsilon,\varphi^\varepsilon)$ be a sequence of minimizers. The boundedness of the $\{(\phi^\varepsilon,\mathbf{p}^\varepsilon)\}$ in $L^\infty(\Omega)$ means that there exists a subsequence, not relabeled, and $(\bar\phi,\bar{\mathbf{p}}) \in L^\infty$ such that

$$\phi^\varepsilon \overset{*}{\rightharpoonup} \bar\phi, \text{ and } \operatorname{supp}(\bar\phi) \subset \Omega,$$
$$\mathbf{p}^\varepsilon \overset{*}{\rightharpoonup} \bar{\mathbf{p}}, \text{ and } \operatorname{supp}(\bar{\mathbf{p}}) \subset \Omega.$$

From (16) and lemma 5.1, we get

$$\int_{\mathbf{R}^2} \bar{\mathbf{p}} \cdot \nabla\eta \, d\mathbf{x} = 0, \text{ for } \eta \in C_0^\infty(\mathbf{R}^2). \tag{17}$$

Let $(\mu_{\mathbf{x}})_{\mathbf{x}\in\Omega}$ be a Young measure generated by $\{(\phi^\varepsilon,\mathbf{p}^\varepsilon)\}$. By properties of Young measure [27], we get

$$(\bar\phi(\mathbf{x}),\bar{\mathbf{p}}(\mathbf{x})) = \int_{\mathbf{R}^2} (\phi,\mathbf{p}) \, d\mu_{\mathbf{x}}(\phi,\mathbf{p}),$$
$$\int_\Omega f(\bar\phi,\bar{\mathbf{p}}) \, d\mathbf{x} = \int_\Omega \int_{\mathbf{R}^2} f(\phi,\mathbf{p}) \mu_{\mathbf{x}}(\phi,\mathbf{p}) \, d\mathbf{x}.$$

Since $f(\phi^\varepsilon,\mathbf{p}^\varepsilon) \to 0$ as $\varepsilon \to 0$,

$$\int_{\mathbf{R}^2} f(\phi,\mathbf{p}) \, d\mu_{\mathbf{x}}(\phi,\mathbf{p}) = 0.$$

This implies that $\operatorname{supp}(\mu_{\mathbf{x}}) \subset \{(-\pi/2,\mathbf{e}_1),(\pi/2,-\mathbf{e}_1)\}$, and

$$\mu_{\mathbf{x}} = \lambda(\mathbf{x})\delta_{(-\pi/2,\mathbf{e}_1)} + (1-\lambda(\mathbf{x}))\delta_{(\pi/2,-\mathbf{e}_1)}.$$

From (17), we obtain

$$0 = \int_{\mathbf{R}^2} \bar{\mathbf{p}} \cdot \nabla\eta \, d\mathbf{x} = \int_{\mathbf{R}^2} (2\lambda(\mathbf{x}) - 1)\mathbf{e}_1 \chi_\Omega \cdot \nabla\eta \, d\mathbf{x}, \text{ for all } \eta \in C_0^\infty(\mathbf{R}^2).$$

In other words, we have

$$\int_{\mathbf{R}^2} (2\lambda(\mathbf{x}) - 1)\chi_\Omega \frac{\partial\eta}{\partial x_1} \, d\mathbf{x} = 0, \text{ for all } \eta \in C_0^\infty(\mathbf{R}^2),$$

and thus $(2\lambda(\mathbf{x}) - 1)\chi_\Omega$ is independent of x_1. Since its support is in Ω,

$$2\lambda(\mathbf{x}) - 1 = 0 \text{ for all } \mathbf{x} \in \Omega.$$

Therefore we get

$$\mu_{\mathbf{x}} = \frac{1}{2}\delta_{(-\pi/2,\mathbf{e}_1)} + \frac{1}{2}\delta_{(\pi/2,-\mathbf{e}_1)}.$$

□

From the above analysis, we observe that if the ratio of elastic constant K to the domain size L approaches to zero, the minimizer of the limiting energy is a Young measure with equal probabilities of two uniform states.

6. **Near the transition from the SmA phase to the ferroelectric SmC.** In this section, we discuss switching problems between uniform states by an externally applied field in a one dimensional problem. We ignore the electrostatic energy and obtain a simplified version of the energy.

Assume that equilibrium configurations are independent of y, and that the system satisfies the following ansatz:

$$\begin{cases} \tau = \gamma_0 = 0,\ \omega_n < 0,\ \omega_p = 0,\ \omega_r > 0,\ \chi_0 = \sin\theta_c \cos\theta_c, \\ d_1 < \theta_c << 1,\ d_2 = d_3 = 1,\ \frac{\partial \mathbf{n}}{\partial \nu} = \frac{\partial \mathbf{P}}{\partial \nu} = 0 \text{ on } z = 0, 1. \end{cases} \tag{18}$$

It follows that the ground states of the energy $\mathcal{E}$ (without the surface energy) is given by

$$\begin{cases} \mathbf{n} = (\sin[\theta_c u_c]\cos\phi, \sin[\theta_c u_c]\sin\phi, \cos[\theta_c u_c]), \\ \mathbf{P} = \pm\left(\frac{1}{2}\sin[2\theta_c u_c]\right)(\sin\phi, -\cos\phi, 0), \end{cases} \tag{19}$$

where $\theta_c > 0$ is the fixed angle between $\mathbf{n}$ and the normal vector to smectic layers, $u_c = \pm 1$, and ϕ is the angle between $\mathbf{e}_1$ and $\mathbf{n} - (\mathbf{n}\cdot\mathbf{e}_3)\mathbf{e}_3$ (the projection of $\mathbf{n}$ onto the xy plane). Since $d_1 << 1$, the surface anchoring energy F_S is so strong that the angle ϕ is close to $\pm\frac{\pi}{2}$. This leads us to assume that $\phi = \pm\frac{\pi}{2}$. This is known as surface-stabilized ferroelectric liquid crystals (SSFLC) [19, pp. 67].

From the bulk energy, the part of the total energy which dominates on the interface between $u = 1$ and $u = -1$ is

$$K|\nabla \mathbf{n}|^2 + Dq^2(\nabla\cdot\mathbf{n})^2 + B|\nabla\mathbf{P}|^2 + g(\mathbf{P}) - \mathbf{P}\cdot\mathbf{E},$$

where $\mathbf{E} = (E_a, 0, 0)$ is an applied field and

$$\begin{cases} \mathbf{n} = (0, \sin[\theta_c u(z)], \cos[\theta_c u(z)]), \\ \mathbf{P} = \frac{1}{2}(\sin[2\theta_c u(z)])(1, 0, 0). \end{cases}$$

Denote

$$\frac{\delta^2}{2} = \frac{(K\theta_c^2 + Dq^2\theta_c^2 + B\theta_c^2)\xi^2}{P_0^r},\quad E = \frac{\xi^2 E_a}{P_0^{r-1}},\quad \alpha = \frac{\gamma}{P_0^4},$$

where $P_0 = \frac{1}{2}\sin[2\theta_c]$ and $r = 4$ for ferroelectric phases while $r = 6$ corresponds to antiferroelectric phases. We approximate $\cos[\theta_c u]$ and $\mathbf{P}\cdot\mathbf{E}$ by 1 and $P_0 E_a u$ respectively (since $\theta_c << 1$). Multiplying $\mathcal{E}$ by $\frac{\xi^2}{P_0^r}$, we obtain the reduced energy functional (still labeled $\mathcal{E}$)

$$\mathcal{E}(u) = \int_0^1 \left\{\frac{\delta^2}{2}(u'(z))^2 + f(u) - Eu\right\} dz, \tag{20}$$

where

$$f(u) = \begin{cases} \frac{1}{4}(u^2-1)^2 & \text{for ferroelectric phases,} \\ \frac{1}{6}u^2\left[(u^2-1)^2 - \alpha\right] & \text{for antiferroelectric phases.} \end{cases} \tag{21}$$

In the antiferroelectric phases, in the absence of applied fields, the free energy of $u = 0$ is smaller than the free energies of $u = \pm 1$ if $\alpha < 0$. In this case, an applied electric field along the positive $x-$axis lowers the free energy of $u = 1$ and switching to $u = 1$ takes place when E reaches critical fields. If α is a negative large number, then removal of the applied filed results in a reorientation of molecules to stabilize the system and switching to $u = -1$ occurs upon application of the field of opposite sign. In this way, the switching between two ferroelectric states is faster than the bistable switching in ferroelectrics. This switching is known as *tristable switching*. The problem (20) also appears in the Landau-Devonshire model of ferroelectric solids, particularly materials in the perovskite family, although the role of the polarization in a ferroelectric solid is different from that of a ferroelectric liquid crystal. In antiferroelectric phase, it can be shown [24] that the problem (20) with the Neumann boundary condition $u'(0) = u'(1) = 0$ exhibits a static hysteresis loop, whose schematic picture is shown in Figure 2 with some appropriate values of α and δ. This agrees qualitatively with experimental data obtained in [3].

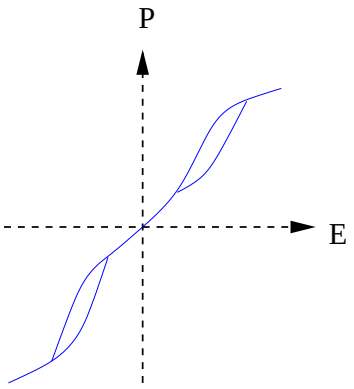

FIGURE 2. Hysteresis between polarization and applied field

7. **Numerical approximations of the switching problems.** In the present section, we study the effects of impurities or thermal noise on the switching problem between two uniform state $u_\pm = \pm 1$ near the phase transition from the smectic A to the smectic C. In the case that $\alpha < 0$, we know $f(0) < f(\pm 1)$. So, if energy barriers between $u = 0$ and $u_\pm = \pm 1$ are small, the molecules tend to reorient and the system starts to relax slowly to the ground state of antiferroelectric phases so as to lower the free energy. In this case, presence of impurities or thermal noise in the system may come into play in the switching. In this section we consider

$$\begin{cases} u_t = \delta u_{xx} - \frac{1}{\delta} f'(u) + \sqrt{\varepsilon}\eta \text{ in } [0,1], \\ u(0,t) = -1, \qquad u(1,t) = 1, \end{cases} \tag{22}$$

where $\varepsilon > 0$ and η is a space-time Gaussian white noise with covariance

$$< \eta(x,t), \eta(y,s) >= \delta(x-y)\delta(t-s),$$

with the Dirac delta $\delta(\cdot)$ as considered in [10].

Notice that the two uniform states $u_\pm = \pm 1$ does not satisfy the boundary conditions $u_\pm(\pm 1) = \pm 1$ in (22). To overcome this difficulty, we replace them by

two approximate solutions, cf. Figure 3, of

$$\delta u_{xx} - \frac{1}{\delta} f'(u) = 0, \quad u(0) = -1, \quad u(1) = 1. \tag{23}$$

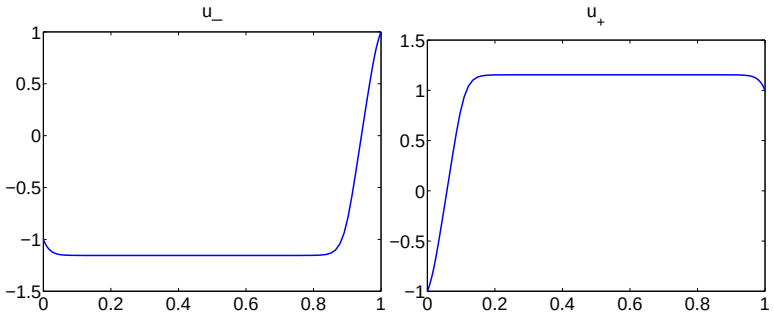

FIGURE 3. Two boundary layer solutions of (23) for antiferroelectrics

By the theory of Wentzell-Freidlin [11], the switching from u_+ to u_- can be understood by the minimization of the action functional

$$\begin{cases} \min\{S_T[u] : u|_{t=0} = u_+, u|_{t=T} = u_-, u|_{x=0} = -1, u|_{x=1} = 1\}, \\ S_T[u] = \int_0^T \int_0^1 \left[u_t - \delta u_{xx} + \frac{1}{\delta} f'(u)\right]^2 dx\, dt. \end{cases} \tag{24}$$

The solution of the above minimization problem represents the optimal switching path between u_+ and u_- in the sense that the probabilities of switching through other paths are exponentially small. The probability of the switching is approximately $e^{-S_T[u]/\delta}$ if u is a minimizer of the problem (24). The sharp interface limit of the action minimization for Allen-Cahn equation is studied in [18]. In [10], the authors studied the optimal switching paths in such systems using the L-BFGS method [29], which is an implementation of a limited memory quasi-Newton method for the nonlinear minimization, coupled with a finite difference discretization in space and time. We shall take a similar approach but with a spectrally accurate Legendre collocation discretization in space and time.

7.1. **Numerical scheme.** We now present our numerical scheme for (24) using a Legendre collocation method for the space-time discretization and the L-BFGS method for nonlinear minimization.

Let us first describe the Legendre collocation method (cf. for instance [5]) for approximating the functional $S_T[u]$. To this end, we transform both the time interval $[0, T]$ and the spatial interval $[0, 1]$ to the standard interval $[-1, 1]$. By setting

$$\tilde{x} = 2x - 1 \in [-1, 1], \tag{25}$$

$$\tilde{t} = \frac{2t}{T} - 1 \in [-1, 1], \tag{26}$$

we rewrite $S_T[u]$ as

$$S_T[u] = \frac{T}{4} \int_{-1}^{1} \int_{-1}^{1} \left(\frac{2}{T} u_t - 4\delta u_{xx} + \delta^{-1} f'(u)\right)^2 dx dt, \tag{27}$$

where, for the sake of notational simplicity, we still use x, t to denote $\tilde{x}$, $\tilde{t}$, and $u(x, t)$ to denote the transformed function.

Given a pair of integers (N, M), we denote $P_{NM} = P_N \times P_M$ where P_N (resp. P_M) is the space of polynomials of degree less or equal than N (resp. M). Let $\{x_i\}_{i=0}^N$ and $\{t_j\}_{j=0}^M$ be the Legendre-Gauss-Lobatto points in x and t. We set $u_{N,\pm}(x) = \sum_{i=0}^N u_\pm(x_i) h_i^N(x)$ which are the interpolating polynomials of $u_\pm$ based on $\{x_i\}_{i=0}^N$. Let

$$G(u) = \frac{2}{T} u_t - 4\delta u_{xx} + \delta^{-1} f'(u), \tag{28}$$

and set

$$X_{NM} = \{u \in P_{NM} : u|_{t=\pm 1} = u_{N,\pm}(x),\ u|_{x=\pm 1} = \pm 1\}, \tag{29}$$

our discrete minimization problem is:

$$\min_{u_{NM} \in X_{NM}} S_T[u_{NM}] = \min_{u_{NM} \in X_{NM}} \frac{T}{4} \sum_{i=0}^N \sum_{j=0}^M G_{ij}^2 \omega_i^N\, \omega_j^M \tag{30}$$

where $G_{i,j} = G(u_{NM}(x_i, t_j))$, and ω_i^N, ω_j^M are the weights of the Legendre-Gauss-Lobatto quadratures associated with $\{x_i\}_{i=0}^N$ and $\{t_j\}_{j=0}^M$, respectively.

Now let us denote by $h_i^N(x)$ and $h_j^M(t)$ the Lagrange polynomials associated with $\{x_i\}_{i=0}^N$ and $\{t_j\}_{j=0}^M$. We can then write

$$u_{NM}(x,t) = \sum_{i=0}^N \sum_{j=0}^M u_{NM}(x_i, t_j) h_i^N(x) h_j^M(t) \in P_{NM}.$$

To simplify the notation, we write $v_{ij} = u_{NM}(x_i, t_j)$. The derivatives of u_{NM} at the collocation points (x_i, t_j) can be computed directly and exactly as follows:

$$\begin{aligned} v_{ij}^t &:= \frac{\partial}{\partial t} u_{NM}(x_i, t_j) = \sum_{m=0}^M v_{im} \frac{d}{dt} h_m^M(t_j), \\ v_{ij}^{xx} &:= \frac{\partial^2}{\partial x^2} u_{NM}(x_i, t_j) = \sum_{n=0}^N v_{nj} \frac{d^2}{dx^2} h_n^N(x_i). \end{aligned} \tag{31}$$

The formulas of $\frac{d}{dt} h_k^M(t_j)$ and $\frac{d^2}{dx^2} h_k^N(x_i)$ can be found, for example, in [5].

For $u_{NM} \in X_{NM}$, we have $v_{i0} = u_-(x_i)$, $v_{iM} = u_+(x_i)$ and $v_{0j} = -1$, $v_{Nj} = 1$. Hence, the unknowns are $\{v_{ij}\}_{1 \le i \le N-1,\, 1 \le j \le M-1}$.

In order to apply the L-BFGS method, we need to compute $\frac{\partial S_T[u_{NM}]}{\partial v_{kl}}$ for $1 \le k \le N-1$, $1 \le l \le M-1$. We derive from (30)

$$\frac{\partial S_T[u_{NM}]}{\partial v_{kl}} = \frac{T}{2} \sum_{i=0}^N \sum_{j=0}^M \omega_i^N \omega_j^M G_{ij} \frac{\partial G_{ij}}{\partial v_{kl}}. \tag{32}$$

The last term in the summation can be computed as follows:

From (28) and (31), we obtain that

$$\begin{aligned} \frac{\partial G_{ij}}{\partial v_{kl}} &= \frac{2}{T} \frac{\partial v_{ij}^t}{\partial v_{kl}} - 4\delta \frac{\partial v_{ij}^{xx}}{\partial v_{kl}} + \delta^{-1} \frac{\partial f'(v_{ij})}{\partial v_{kl}} \\ &= \frac{2}{T} \delta_{ik} \frac{d}{dt} h_l^M(t_j) - 4\delta_{jl} \frac{d^2}{dx^2} h_k^N(x_i) + \delta^{-1} \frac{\partial f'(v_{ij})}{\partial v_{kl}} \end{aligned} \tag{33}$$

where δ_{ik} and δ_{jl} are Kronecker delta functions. Since $f'(u) = \frac{1}{3}(3u^5 - 4u^3 + (1-\alpha)u)$, we have

$$\frac{\partial f'(v_{ij})}{\partial v_{kl}} = \frac{1}{3} \delta_{ik} \delta_{jl} (15 v_{kl}^4 - 12 v_{kl}^2 + (1-\alpha)). \tag{34}$$

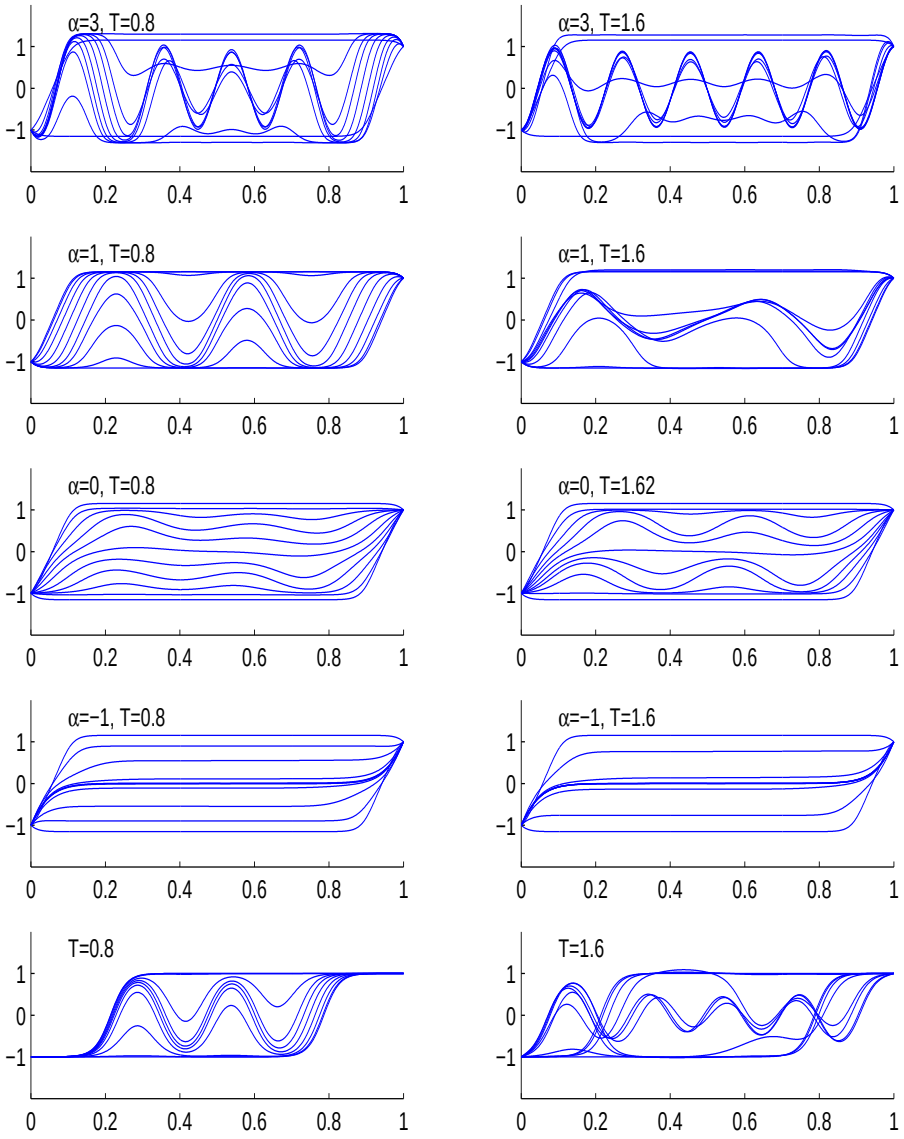

FIGURE 4. Switching patterns between the two states $u_{\pm}$

Hence, for given u_{NM}, the partial derivatives $\frac{\partial S_T[u_{NM}]}{\partial v_{kl}}$ with $1 \le k \le N-1$, $1 \le l \le M-1$ can be efficiently computed with spectral accuracy, so we can use the L-BFGS algorithm to solve the discrete minimization problem (30).

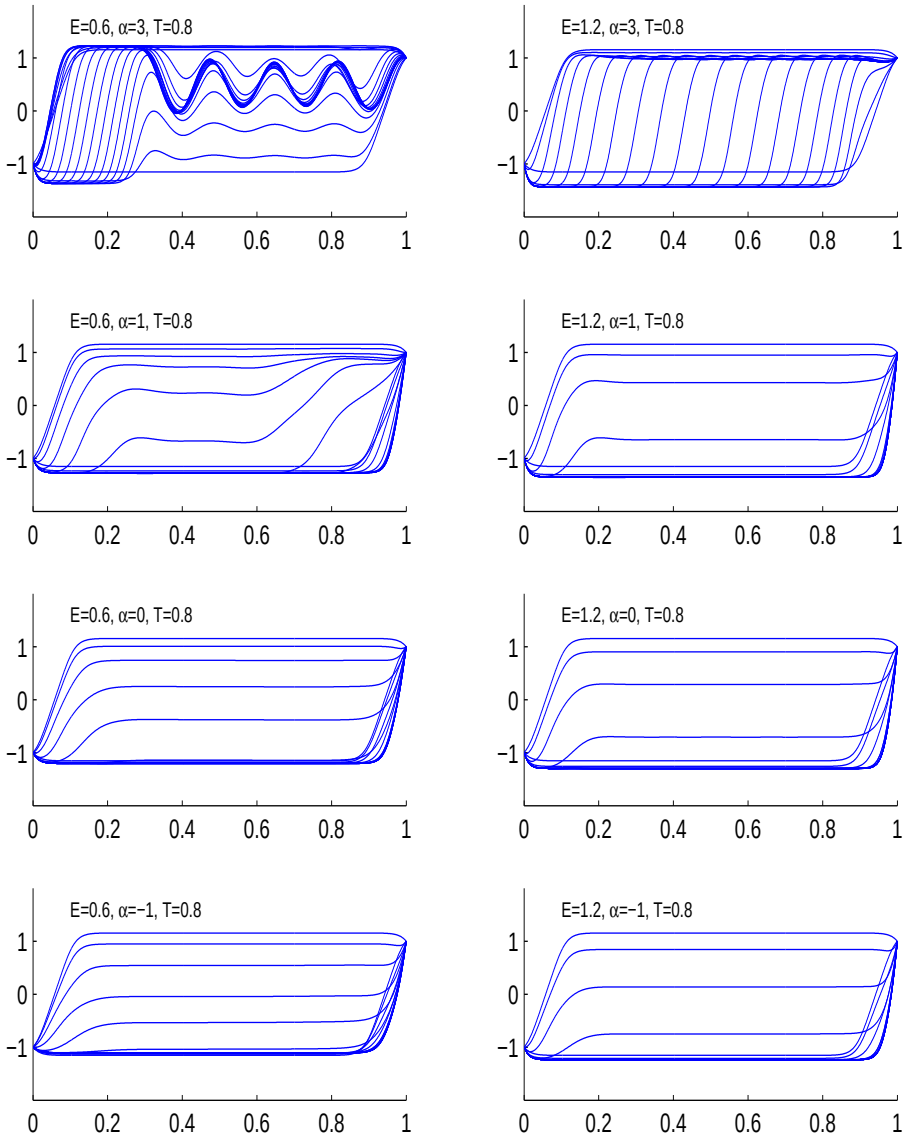

FIGURE 5. Switching patterns between the two states $u_{\pm}$ with respect to impurities and a small applied field

7.2. **Numerical results.** We now present some numerical simulation for the switching problem. The numerical parameters used for these simulations are $N = 80$ and $M = 40$. To ensure that converged solutions are obtained, we have also used a larger pair of (N, M) and obtained virtually identical results.

In Figure 4, we plot the simulated switching patterns between the two states $u_\pm$. Switchings in antiferroelectrics are represented in the first four rows from the top and nucleations of periodic solutions appear during the polarization reversal process. Since $u = 0$ is a local minimizer of $f(u)$, we see that almost all switchings, except the case $\alpha = 1$ and $T = 0.8$, pass through $u = 0$ for the most part of the interval $[0, 1]$. Note that if $\alpha < 0$ then $f(0) < f(\pm 1)$. This explains why u stays loner near the state 0 for the case $\alpha = -1$. However, for $\alpha > 0$, we have $f(0) > f(\pm 1)$. So u is not expected to stay as long near the state 0 (cf. the first two rows in Fig. 4) as in the case $\alpha < 0$. In this case, switching undergoes nucleations since energy barrier between $u = 0$ and $u = \pm 1$ is getting larger. These simulations indicate that the switching is faster with smaller α when $\alpha > 0$, which is consistent with the fact that a smaller value of α leads to a smaller energy barrier between 0 and ± 1.

When we increase the switching time T from 0.8 to 1.6, we observe that all switchings go near the state $u = 0$ for the first four rows from the top (antiferroelectrics). For $\alpha > 0$, switching for $T = 1.6$ also seems to go through nucleations, but it produces slightly milder oscillations. Similarly, we can expect that when we decrease the switching time (say from $T = 0.8$ to $T = 0.1$), more nucleations will take place for the switching to occur. It should be noted that the switching we study here is a rare event and the probability of the switching is very low.

As a comparison, we plot in the last row of Figure 4 the switching process between two solutions $u_\pm$ satisfying (23) for ferroelectrics, where $f(u) = \frac{1}{4}(1 - u^2)^2$ is the double well potential. There appears to be more oscillations instead of having a plateau near $u = 0$. In this case, the switching proceeds by nucleations. We refer the reader to [10, 18] for more detail in this regard.

Next, we study the optimal switching patterns with respect to impurities and a small applied field E. To this end, we substitute $f(u)$ by $f(u) + Eu$ with a constant field E and consider only antiferroelectrics. We plot in Figure 5 the switching patterns from u_+ to u_- (see Figure 3) upon application of an electric field $-E(E > 0)$. It appears that switching proceeds faster as we decrease the values of α and most of switchings do not nucleate bumps except in the case that $\alpha = 3$ and $T = 0.8$. Increasing the strength of E appears to make the switching faster. For a small electric field, it is expected that nucleations will also occur during the switching when we decrease the switching time.

8. **Numerical simulation of minimum configurations.** In this section, we study local minimizers of the energy in a one-dimensional problem. In particular, we investigate the role of spontaneous twist and bend in the minimum configurations. Let $\mathbf{n}$ and $\mathbf{p}$ be periodic functions depending only on z and satisfy

$$\mathbf{n} = (au_1, au_2, c), \quad \mathbf{p} = (q_1, q_2, 0), \; u_1^2 + u_2^2 = 1.$$

The energy functional we consider is

$$\int_0^L F(\mathbf{u}, \mathbf{q})\, dz,$$

where $\mathbf{u} = (u_1, u_2)$, $\mathbf{q} = (q_1, q_2)$ and

$$\begin{aligned} F &= \frac{1}{K}(F_{Sm} + F_N + F_P - K\tau^2) \\ &= a^2 \left|\frac{d\mathbf{u}}{dz}\right|^2 + \frac{L_1}{2}\left|\frac{d\mathbf{q}}{dz}\right|^2 + L_2\mathbf{u}\cdot\left(-\frac{du_2}{dz}, \frac{du_1}{dz}\right) + L_3\mathbf{q}\cdot\frac{d\mathbf{u}}{dz} + \gamma_0^2 P_0^2|\mathbf{q}|^2 \\ &\quad + L_4\left[a^2c^2(u_2q_1 - u_1q_2)^2 - \chi_0^2|\mathbf{q}|^2\right]^2 + \frac{1}{\bar{\epsilon}^2}(|\mathbf{u}|^2 - 1)^2 + \frac{1}{4\bar{\eta}^2}(|\mathbf{q}|^2 - 1)^2, \end{aligned}$$

with

$$\begin{aligned} &L_1 = \frac{2BP_0^2}{K}, \quad L_2 = 2a^2\tau, \quad L_3 = 2ac\gamma_0 P_0, \quad ac = \chi_0, \\ &L_4 = \frac{K_c k^8 P_0^4}{2K}, \quad \bar{\epsilon}^2 = \frac{K\epsilon^2}{a^4}, \quad \bar{\eta}^2 = \frac{K\eta^2}{P_0^4}. \end{aligned}$$

For numerical simulations, we let γ_0 vary from -3 to 3 and set

$$\begin{aligned} &a = \sin 30^\circ, \quad \tau = 2a^2, \quad 2B = K, \; P_0 = 1, \quad L_4 = 5, \\ &a^2c^2 = \chi_0^2, \quad \frac{1}{\bar{\epsilon}^2} = 4, \quad \frac{1}{4\bar{\eta}^2} = 10. \end{aligned}$$

We use L-BFGS to approximate local minimizers of the energy functional $\int_0^L F(\mathbf{u}, \mathbf{q})\, dz$ with $L = 2\pi$. Since $\mathbf{u}$ and $\mathbf{q}$ are periodic functions, we use a Fourier collocation method (cf. [5]) to approximate the function. The setup of the Fourier-collocation method is similar to the procedure for setting up the Legendre-collocation method presented in the last section so we omit the detail here.

In the simulations, we introduce two different sets of initial guesses to find different local minimizers. One is given by

$$\begin{cases} \mathbf{u}_0 = \left(\cos\frac{\tau z}{a^2}, \sin\frac{\tau z}{a^2}\right), \; \mathbf{u}_0(z) = \mathbf{u}_0(L), \\ \mathbf{q}_0(z) = \left(\sin\frac{\tau z}{a^2}, -\cos\frac{\tau z}{a^2}\right), \mathbf{q}_0(0) = \mathbf{q}_0(L). \end{cases} \tag{35}$$

With this initial guess, we obtain a pair of nontrivial periodic functions $(\mathbf{u}_{per}, \mathbf{q}_{per})$ as a local minimizer for $\int_0^L F\, \mathrm{dz}$.

The other set of initial guess is given by

$$\begin{cases} \mathbf{u}_0 = \left(0.06\cos\frac{\tau z}{a^2}, 0.06\sin\frac{\tau z}{a^2} + 0.5\right), \; \mathbf{u}_0(z) = \mathbf{u}_0(L), \\ \mathbf{q}_0(z) = \left(0.06\sin\frac{\tau z}{a^2} + 0.5, -0.06\cos\frac{\tau z}{a^2}\right), \mathbf{q}_0(0) = \mathbf{q}_0(L). \end{cases} \tag{36}$$

We obtain a pair of constant functions $(\mathbf{u}_c, \mathbf{q}_c)$ as a local minimizer.

In Figure 6, we plot energies for $(\mathbf{u}_{per}, \mathbf{q}_{per})$ and $(\mathbf{u}_c, \mathbf{q}_c)$ with respect to $\gamma_0 \in [-3, 3]$. The dotted curve is the energy for $(\mathbf{u}_{per}, \mathbf{q}_{per})$ with γ_0 varying from -3 to 3 while the solid curve is the one for $(\mathbf{u}_c, \mathbf{q}_c)$. These graphs explain that constant configurations are preferred if $\gamma_0 \in [-3, s_1) \cup (s_2, 3]$, where s_1 is a constant in $(-2.35, -2.3)$ and s_2 is close to 0.6 as in Figure 7. For $\gamma_0 \in (s_1, s_2)$, energies for periodic solutions are smaller than those for constant solutions. The energies for constant and periodic solutions are denoted by two small boxes on the curves when $\gamma_0 = \frac{c\tau}{a} = \sin 60^\circ$ in Figure 6. In this case, it is observed in the literature that spontaneous twist and bend contribute equally in the system, resulting in an unwounded state, i.e. constant configuration [8, pp. 384]. Our results also show that the unwounded state remains for $\gamma_0 \in (s_1, s_2)$, $\frac{a\tau}{c} < s_2$.

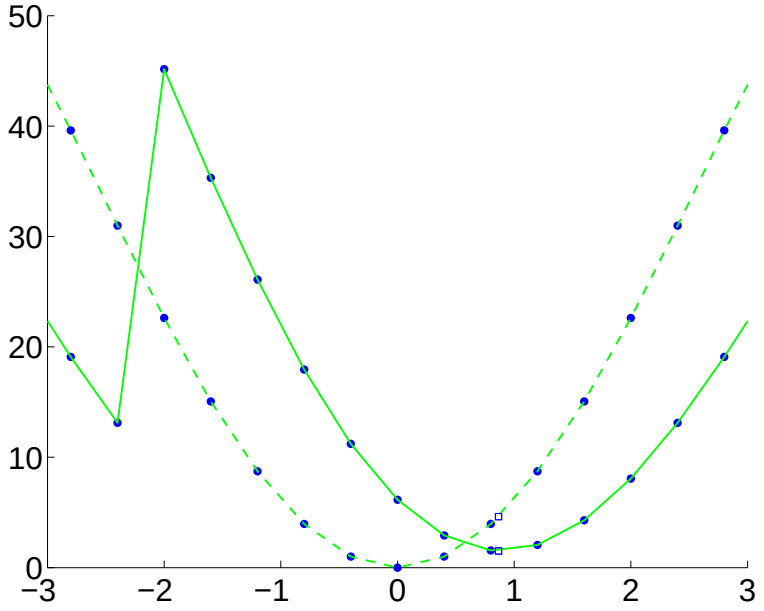

FIGURE 6. Energies for constant (solid curve) and periodic (dotted curve) solutions for $-3 \leq \gamma_0 \leq 3$

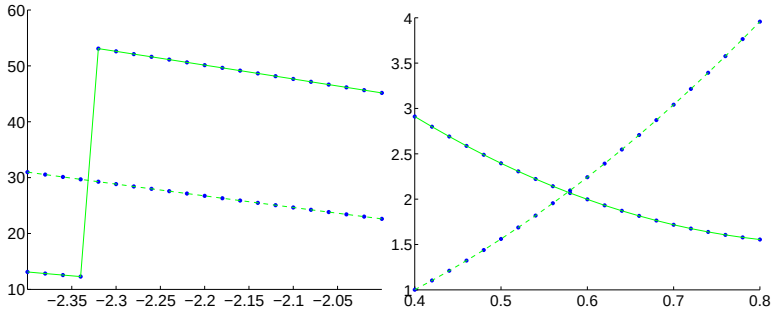

FIGURE 7. Left: $-2.35 < s_1 < -2.3$, right: $0.5 < s_2 < 0.6$

9. **Conclusion.** We presented in this paper a modeling and simulation of ferroelectric liquid crystals accounting for antiferroelectric phases.

We studied, in the case of bookshelf geometry in connection with a SSFLC, the existence of multi-phases with sharp interfaces in the system by means of bifurcation and Young measure arguments. In the vicinity of the phase transition between the SmA phase and ferroelectric SmC, we showed that the present model exhibits hysteresis loops between polarization and applied field. This agrees qualitatively with early experimental data reported in [3].

By adding stochastic noise to the problem, so as to model the inclusion of impurities, we simulated optimal switching pattern by using the L-BFGS method coupled with a spectral discretization in space and time. We studied switching patterns with respect to the time and a parameter α depending on a_1, a_{11}, a_{111} (cf. 21). Our numerical results reveals that the switching between two ferroelectric states tends

to antiferroelectric state, due to the antiferroelectric potential. In the absence of stochastic noise, we observed from our numerical simulations that the competition between twist and bending terms leads to periodic structures and there exists regimes in which either constant or periodic states are favored.

We carried out numerical approximations to local minimizers with an emphasis on the role of spontaneous twist and bend. We found that, although molecules in the SmC^* phase tend to be aligned in a helical pattern, the helical structure can be suppressed due to the competition between them. We also investigated energy landscape with respect to various coefficients in the energy functional.

Acknowledgments. The authors would like to thank the referees for their careful reading of the manuscript and comments.

REFERENCES

[1] A. Ambrosetti and G. Prodi, "A Primer of Nonlinear Analysis," Cambridge University Press, Cambridge, 1993.
[2] C. Bailey, E. C. Gartland and A. Jákli, *Structure and stability of bent core liquid crystal fibers*, Phys. Rev. E, **75** (2007), 031701.
[3] V. Bourny and H. Ohihara, *Field-induced behaviors near the smectic A–smectic C_α phase transition of an antiferroelectric liquid crystals*, Phys. Rev. E, **63** (2001), 021703.
[4] W. Cao and L. E. Cross, *Theory of tetragonal twin structures in ferroelectric perovskies with a first order transition*, Phys. Rev. B, **44** (1991), 44.
[5] C. Canuto, M. Y. Hussaini, A. Quarteroni and T. A. Zang, "Spectral Methods in Fluid Dynamics," Springer-Verlag, New York, 1987.
[6] G. Chen, S. Ding, C.-R. Hu, W.-M. Ni and J. Zhou, *A note on the elliptic Sine-Gordon equation*, in Variational Methods: Open Problems, Recent Progress, and Numerical Algorithms, Contemp. Math., J. M. Neuberger, ed., Amer. Math. Soc., Providence, RI, **357** (2004), 49–67.
[7] J. Chen and T. C. Lubensky, *Landau-Ginzburg mean-field theory for the nematic to smectic C and nematic to smectic A liquid crystal transistions*, Phys. Rev. A, **14** (1976), 1202–1297.
[8] P. G. de Gennes and J. Prost, "The Physics of Liquid Crystals," Clarendon Press, Oxford, 1993.
[9] Z. Ding, G. Chen and S. Li, *On positive solutions of the elliptic Sine-Gordon equation*, Commun. Pure Appl. Anal., **4** (2005), 283–294.
[10] W. E, W. Ren and E. Vanden-Eijnden, *Minimum action method for the study of rare events*, Comm. Pure Appl. Math., **57** (2004), 637–656.
[11] M. I. Freidlin and A. D. Wentzell, "Random Perturbations of Dynamical Systems," Springer-Verlag, 1998.
[12] M. Golubitsky and D. G. Schaffer, "Singularities and Groups in Bifurcation Theory. volume **I**," Springer-Verlag, New York, 1985.
[13] M. A. Handschy and N. A. Clark, *Structures and responses of ferroelectric liquid crystals in the surface-stabilized geometry*, Ferroelectrics, **59** (1984), 69–116.
[14] A. Jákli, C. Bailey and J. Harden, "Thermotropic Liquid Crystals," Springer, 2007.
[15] A. Jákli, T. Kósa, A. Vajda, E. Benkler, I. Jánossy and P. Palffy-Muhoray, *Optically induced periodic structures in smectic-C liquid crystals*, Phys. Rev. E, **63** (2000), 011705.
[16] R. D. James and D. Kinderlehrer, *Frustration in ferromagnetic materials*, Cont. Mech. Thermodynamics, **2** (1990), 215–239.
[17] K. Kang and J. Park, *A partial regularity of static configurations in ferroelectric liquid crystals*, in preparation.
[18] R. V. Kohn, M. G. Reznikoff and Y. Tonegawa, *Sharp-interface limit of the Allen-Cahn action functional in one space dimension*, Calc. Var. Partial Differential Equations, **25** (2006), 503–534.
[19] S. T. Lagerwall, "Ferroelectric and Antiferroelectric Liquid Crystals," Wiley-VCH, 1999.
[20] I. Lukyanchuk, *Phase transition between the cholesteric and twist grain boundary C phases*, Phys. Rev. E, **57** (1998), 574–581.

[21] P. Mach, R. Pindak, A. M. Levelut, P. Barois, H. T. Nguyen, C. C. Huang, and L. Furenlid, *Structural chrarateriza tion of various chiral Smectic-C phases by resonant X-ray scattering*, Phys. Rev. Lett., **81** (1998), 1015.
[22] I. Muševič, R. Blinc and B. Žekš, "The Physics of Ferroelectric and Antiferroelectric Liquid Crystals," World-Scientific, Singapore, New Jersey, London, Hong Kong, 2000.
[23] M. A. Osipov and S. A. Pikin, *Dipolar and quadrapolar ordering in ferroelectric liquid crystals*, J. Phys. II France, **5** (1995), 1223–1240.
[24] J. Park, *Existence of finitely many solution branches and nested hysteresis loops in ferroelectric materials*, preprint.
[25] J. Park and M. C. Calderer, *Analysis of nonlocal electrostatic effects in chiral smectic c liquid crystals*, SIAM J. Appl. Math., **66** (2006), 2107–2126.
[26] S. Pikin, "Structural Transformations in Liquid Crystals," Gordon and Breach Science Publishers, New York, 1991.
[27] L. Tartar, *Compensated compactness and applications to partial differential equations*, Res. Notes in Math., **39** (1979), 136–212.
[28] D. M. Walba, "Topics in Stereochemistry," vol. **24**, John Wiley & Sons, Inc., 2003.
[29] C. Zhu, R. H. Byrd and J. Nocedal, *L-BFGS-B: Algorithm 778: L-BFGS-B, FORTRAN subroutines for large scale bound constrained optimization*, ACM Trans. Math. Soft., **23** (1997), 550–560.

Received January 2009; revised June 2009.

E-mail address: park196@math.purdue.edu
E-mail address: chen221@math.purdue.edu
E-mail address: shen@math.purdue.edu